Acta Crystallographica Section C
Crystal Structure Communications
ISSN 0108-2701

Three transition-metal complexes with the macrocyclic ligand *meso*-5,7,7,12,14,14-hexamethyl-1,4,8,11-tetraazacyclotetradecane (*L*): $[Cu(ClO_4)_2(L)]$, $[Zn(NO_3)_2(L)]$ and $[CuCl(L)(H_2O)]Cl$

Sabina Yasmin, Sebastián Suarez, Fabio Doctorovich, Tapashi G. Roy and Ricardo Baggio

Acta Cryst. (2013). C**69**, 862–867

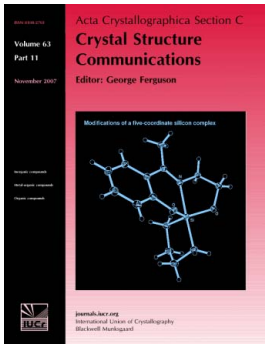

Acta Crystallographica Section C
Crystal Structure Communications
ISSN 0108-2701

Three transition-metal complexes with the macrocyclic ligand *meso*-5,7,7,12,14,14-hexamethyl-1,4,8,11-tetraazacyclotetradecane (*L*): $[Cu(ClO_4)_2(L)]$, $[Zn(NO_3)_2(L)]$ and $[CuCl(L)(H_2O)]Cl$

Sabina Yasmin,[a] Sebastián Suarez,[b]* Fabio Doctorovich,[b] Tapashi G. Roy[a] and Ricardo Baggio[c]

[a]University of Chittagong, Chittagong 4331, Bangladesh, [b]Departamento de Química Inorgánica, Analítica y Química, Física/INQUIMAE–CONICET, Facultad de Ciencias Exactas y Naturales, Universidad de Buenos Aires, Buenos Aires, Argentina, and [c]Gerencia de Investigación y Aplicaciones, Centro Atómico Constituyentes, Comisión Nacional de Energía Atómica, Buenos Aires, Argentina
Correspondence e-mail: seba@qi.fcen.uba.ar

Received 25 June 2013
Accepted 3 July 2013

The three transition-metal complexes, (*meso*-5,7,7,12,14,14-hexamethyl-1,4,8,11-tetraazacyclotetradecane-κ^4N)bis(perchlorato-κO)copper(II), $[Cu(ClO_4)_2(C_{18}H_{40}N_4)]$, (I), (*meso*-5,7,7,12,14,14-hexamethyl-1,4,8,11-tetraazacyclotetradecane-κ^4N)bis(nitrato-κO)zinc(II), $[Zn(NO_3)_2(C_{18}H_{40}N_4)]$, (II), and aquachlorido(*meso*-5,7,7,12,14,14-hexamethyl-1,4,8,11-tetraazacyclotetradecane-κ^4N)copper(II) chloride, $[CuCl(C_{18}H_{40}N_4)(H_2O)]Cl$, (III), are described. The molecules display a very similarly distorted 4+2 octahedral environment for the cation [located at an inversion centre in (I) and (II)], defined by the macrocycle N_4 group in the equatorial sites and two further ligands in *trans*-axial positions [two O–ClO_3 ligands in (I), two O–NO_2 ligands in (II) and one chloride and one aqua ligand in (III)]. The most significant difference in molecular shape resides in these axial ligands, the effect of which on the intra- and intermolecular hydrogen bonding is discussed. In the case of (I), all strong hydrogen-bond donors are saturated in intramolecular interactions, while weak intermolecular C—H···O contacts result in a three-dimensional network. In (II) and (III), instead, there are N—H and O—H donors left over for intermolecular interactions, giving rise to the formation of strongly linked but weakly interacting chains.

Keywords: crystal structure; macrocycles; biologically important compounds; chiral compounds.

1. Introduction

The importance of synthetic macrocyclic complexes is due to their presence in many naturally occurring metal complexes of biological significance, such as haemoglobin, vitamin B12, chlorophyll *etc.*, which play vital roles in biology (Reid & Schroder, 1990; Bernhardt & Lawrance, 1990). Among the

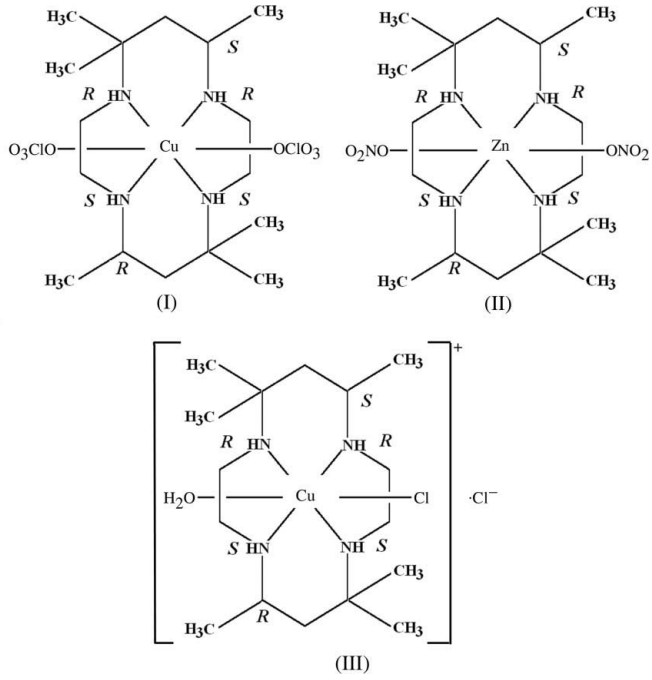

most versatile macrocyclic ligands synthesized, saturated tetraazamacrocycles have a key role, since they are capable of producing inert stable complexes with a number of different metal ions of biomedical importance, a fact which has attracted the interest of chemists due to their impact in various

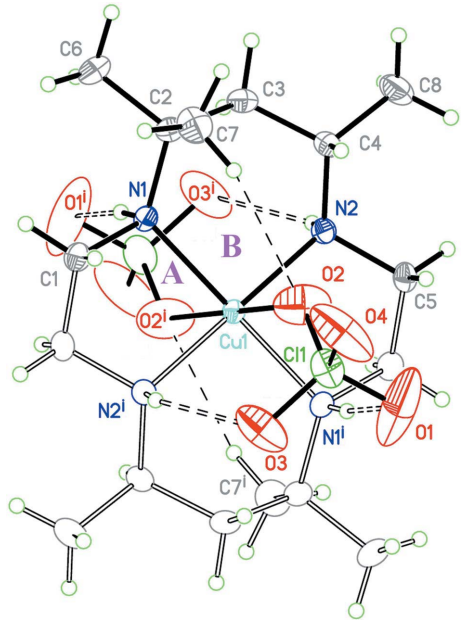

Figure 1
A displacement ellipsoid plot of (I), drawn at the 30% probability level, showing the atom-numbering scheme. Full (empty) ellipsoids represent independent (symmetry-related) atoms. Double (single) broken lines denote conventional (nonconventional) hydrogen bonds. Labels A and B correspond to the $R(6)$ rings defined by the intramolecular N—H···O hydrogen bonds. [Symmetry code: (i) $-x+1, -y+1, -z+1$.]

  doi:10.1107/S0108270113018465

Table 1
Experimental details.

	(I)	(II)	(III)
Crystal data			
Chemical formula	$[Cu(ClO_4)_2(C_{18}H_{40}N_4)]$	$[Zn(NO_3)_2(C_{18}H_{40}N_4)]$	$[CuCl(C_{18}H_{40}N_4)(H_2O)]Cl$
M_r	546.93	473.88	436.94
Crystal system, space group	Monoclinic, $P2_1/n$	Monoclinic, $C2/c$	Monoclinic, $P2_1/c$
Temperature (K)	295	295	295
a, b, c (Å)	8.460 (5), 9.162 (5), 15.506 (5)	12.9252 (9), 11.7664 (5), 15.5628 (10)	14.0350 (4), 11.6288 (2), 13.8132 (4)
β (°)	98.097 (5)	113.352 (8)	111.255 (3)
V (Å^3)	1189.9 (10)	2173.0 (2)	2101.10 (9)
Z	2	4	4
Radiation type	Mo $K\alpha$	Mo $K\alpha$	Mo $K\alpha$
μ (mm^{-1})	1.19	1.17	1.31
Crystal size (mm)	0.22 × 0.20 × 0.16	0.42 × 0.18 × 0.18	0.32 × 0.18 × 0.12
Data collection			
Diffractometer	Oxford Gemini S Ultra CCD area-detector diffractometer	Oxford Gemini S Ultra CCD area-detector diffractometer	Oxford Gemini S Ultra CCD area-detector diffractometer
Absorption correction	Multi-scan (*CrysAlis PRO*; Oxford Diffraction, 2009)	Multi-scan (*CrysAlis PRO*; Oxford Diffraction, 2009)	Multi-scan (*CrysAlis PRO*; Oxford Diffraction, 2009)
T_{min}, T_{max}	0.72, 0.82	0.72, 0.82	0.72, 0.82
No. of measured, independent and observed [$I > 2\sigma(I)$] reflections	15029, 2878, 2167	4791, 2475, 1687	45230, 5230, 4195
R_{int}	0.043	0.032	0.045
$(\sin\theta/\lambda)_{max}$ (Å^{-1})	0.683	0.682	0.684
Refinement			
$R[F^2 > 2\sigma(F^2)]$, $wR(F^2)$, S	0.043, 0.121, 1.08	0.048, 0.127, 1.04	0.039, 0.098, 1.06
No. of reflections	2878	2475	5230
No. of parameters	145	136	235
No. of restraints	21	0	3
H-atom treatment	H-atom parameters constrained	H-atom parameters constrained	H atoms treated by a mixture of independent and constrained refinement
$\Delta\rho_{max}$, $\Delta\rho_{min}$ (e Å^{-3})	0.51, −0.43	0.46, −0.35	0.86, −0.34

Computer programs: *CrysAlis PRO* (Oxford Diffraction, 2009), *SHELXS97* (Sheldrick, 2008), *SHELXTL* (Sheldrick, 2008), *SHELXL97* (Sheldrick, 2008) and *PLATON* (Spek, 2009).

industrial, biochemical and catalytic processes (Kimura *et al.*, 1992, 1994). Metal complexes of the 14-membered tetraaza-macrocyclic ligands, such as the ones reported here, have been studied in radio-immunotherapy and magnetic resonance imaging (Konig *et al.*, 1996; Norman *et al.*, 1995), in pharmacological endeavours (Hollinshead & Smith, 1990) and in crystal engineering (Suh *et al.*, 2006). Among their biologically relevant properties, antifungal (Roy, Hazari, Dey, Meah *et al.*, 2007), antibacterial (Roy, Hazari, Dey, Miah *et al.*, 2007; Roy, Hazari, Dey, Nath *et al.*, 2007) and (in some cases) potential anticancer properties are to be mentioned (Arai *et al.*, 1998; Gao *et al.*, 2010).

The strong sustained research on this subject over the last 50 years has been summarized in a recent review (Curtis, 2012), where a large number of different *N*-substituted (*N*-methyl, *N*-propyl or *N*-allyl) macrocyclic ligands complexed to a variety of cations (*e.g.* Cu, Co, Cr, Zn, Cd and Pd) were analysed.

As part of our interest in macrocyclic complexes, we have recently discussed the slight molecular distortions taking place, and the rather large hydrogen-bonding changes they give rise to, in three Cu^{II} complexes having different isomers of 3,5,7,7,10,12,14,14-octamethyl-1,4,8,11-tetraazacyclotetradecane, *viz*. centrosymmetric L^1, with an *RRRR–SSSS* chiral centre distribution, and noncentrosymmetric L^2 with an *RRRS–SRSR* distribution. These complexes had in common

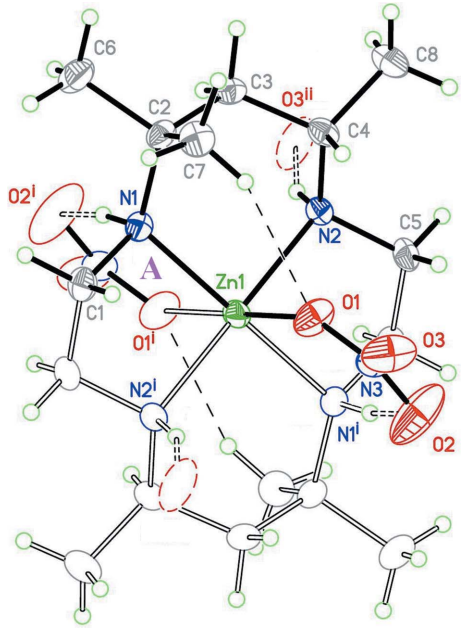

Figure 2
A displacement ellipsoid plot of (II), drawn at the 30% probability level, showing the atom-numbering scheme. Full (empty) ellipsoids represent independent (symmetry-related) atoms. Double (single) broken lines denote conventional (nonconventional) hydrogen bonds. Label A corresponds to the $R(6)$ ring defined by the intramolecular N—H···O hydrogen bond. [Symmetry codes: (i) $-x+\frac{1}{2}, -y+\frac{1}{2}, -z$; (ii) $x+\frac{1}{2}, -y+\frac{1}{2}, z-\frac{1}{2}$.]

two axially coordinated ClO_4 counter-anions (Nath *et al.*, 2013).

We discuss now a different but somewhat related issue: three transition metal (Tr) complexes with one (and the same) hexamethylated ligand closely related to L^1, *viz.* *meso*-5,7,7,12,14,14-hexamethyl-1,4,8,11-tetraazacyclotetradecane (L), but now having different axial ligands, namely $[Cu^{II}(ClO_4)_2(L)]$, (I), $[Zn^{II}(NO_3)_2(L)]$, (II), and $[Cu^{II}Cl(L)(H_2O)]Cl$, (III), and the effect which these ligands have on both the intra- and intermolecular hydrogen-bonding interactions.

At this stage it should be mentioned that some closely related structures to those presented here have already been reported in the literature, though without the detailed hydrogen-bonding analysis mentioned above, which is the main scope of this paper. Among the most relevant we will mention two relatives of (I), an isomorph with Co^{II} instead of Cu^{II} and the same 5,7,7,12,14,14-hexamethyl L ligand (Bakac & Espenson, 1990), and an isostructural variant having the same Cu^{II} cation, but bound to a 5,5,7,12,12,14-hexamethyl isomer of L (Kalita *et al.*, 2011). There is also an isostructural variant of (III), reported by Temple *et al.* (1984), having Cr^{III} instead of Cu^{II} as the central cation and NO_3^- instead of Cl^- as the counter-anion.

2. Experimental

2.1. Synthesis and crystallization

For the synthesis of $[Cu(ClO_4)_2(L)]$, (I), copper(II) perchlorate hexahydrate (0.479 g, 1.0 mmol) and *meso*-5,7,7,12,14,14-hexamethyl-1,4,8,11-tetraazacyclotetradecane dihydrate ($L{\cdot}2H_2O$; 0.320 g, 1.0 mmol) were dissolved separately in hot methanol (50 ml). The colourless ligand solution was added as soon as possible to the blue salt solution while hot. The resulting mixture was allowed to evaporate slowly and dark-blue crystals of (I) separated. These were filtered off and recrystallized from a minimum quantity of aqueous methanol (1:1 *v*/*v*) (yield 0.12 g). The product was again treated with dibromopyridine to prepare the *N*-substituted ligand. However, the final product gave an identical IR spectrum to the initial diperchlorate complex, showing that no *N*-substitution had taken place. Crystals of (II) suitable for X-ray diffraction were grown by slow evaporation of a solution in a solvent mixture of acetonitrile and ethanol in a 1:1 ratio.

For the synthesis of $[Zn(NO_3)_2(L)]$, (II), $L{\cdot}2H_2O$ (0.320 g, 1.0 mmol) and zinc(II) nitrate hexahydrate (0.297 g, 1.0 mmol) were dissolved separately in hot methanol (20 ml) and mixed while hot. The solution was heated in a steam bath and the volume of the solution reduced to 10 ml. The solution was allowed to cool and the white product, (II), was separated from the solution, washed with methanol followed by diethyl ether, and dried in a vacuum desiccator over silica gel. Crystals of (II) suitable for X-ray diffraction were grown by slow evaporation of a solution in a solvent mixture of dimethyl sulfoxide (DMSO) and acetonitrile in a 1:1 ratio.

For the synthesis of $[CuCl(L)(H_2O)]Cl$, (III), (I) (0.541 g, 1.0 mmol) was added to hot methanol (50 ml) and, after dissolution by heating, a blue solution was obtained. A similar procedure was performed with potassium chloride (KCl; 0.224 g, 3.0 mmol), resulting in a colourless solution. A mixture of both solutions gave a blue–violet solution, which was further heated for 30 min on a water bath and filtered to remove potassium perchlorate as a white solid. The resulting filtrate was dried to give a blue–violet product, (III), and cooled to room temperature. After cooling, chloroform (100 ml) was added and the resulting solution stirred. The light-blue–violet chloroform extract was evaporated off to give the stable blue–violet final product, which was cooled and stored in a desiccator over silica gel. Crystals of (III) suitable for X-ray diffraction were grown by slow evaporation of a solution in a solvent mixture of acetonitrile and ethanol in a 1:1 ratio.

2.2. Refinement

Crystal data, data collection and structure refinement details are summarized in Table 1. All three macrocycles present the same *SRS*(*RSR*) chiral centre distribution, in an N1–N2–C4 sequence. C- and N-bound H atoms were found in a difference map, further idealized and finally allowed to ride. Methyl groups were also free to rotate. Water H atoms in (III) posed some problems due to the large displacement parameter for atom O1*W*; they were not clearly seen in the difference map, but the hydrogen-bonding donor–acceptor scheme for O1*W* clearly defined a restrained solid angle for them. The inclusion of an idealized water molecule (O—H = 0.85 Å and H···H = 1.30 Å) ended up with the H atoms lying on clearly positive zones in the difference Fourier map and involved in strong hydrogen bonding, so this treatment of the water molecule as a rigid group was considered adequate. In all

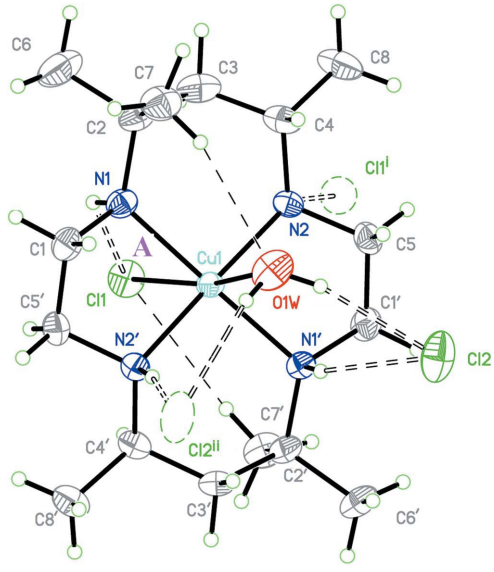

Figure 3
A displacement ellipsoid plot of (III), drawn at the 30% probability level, showing the atom-numbering scheme. Double (single) broken lines denote conventional (nonconventional) hydrogen bonds. Label A corresponds to the $R(4)$ ring defined by the intramolecular N—H···O hydrogen bond. [Symmetry codes: (i) $-x+1, -y+1, -z+1$; (ii) $-x, -y+1, -z+1$.]

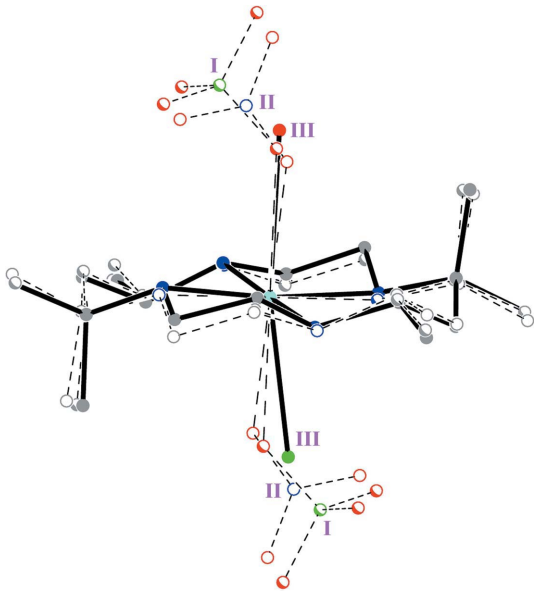

Figure 4
A schematic superposition of (I), (II) and (III), with only the CuN_4 cores included in the least-squares match.

cases, H-atom displacement parameters were taken as $U_{iso}(H) = xU_{eq}$(parent) (methyl C—H = 0.96 Å and x = 1.5; aromatic C—H = 0.93 Å and x = 1.2; N—H = 0.85 Å and x = 1.2; O—H = 0.85 Å and x = 1.5). Some unresolved disorder represented by difference Fourier peaks as high as 0.8 e Å^3 was found near the C2—C3 bond in (III).

3. Results and discussion

Displacement ellipsoid plots for (I), (II), (III) are shown in Figs. 1, 2 and 3, respectively. They present a distorted octahedral disposition around the cation, which in (I) and (II) lie on a centre of inversion, thus rendering only half of the molecule independent. In spite of the cation differences, the chlathrate (*L*)Tr nuclei (Tr = Cu or Zn) are geometrically similar, with a span of the Tr—N distances and *cis*-N—Tr—N angles involving the *L* ligand of, respectively, 2.025 (2)–2.040 (2) Å and 90±4.38 (10)° for (I), 2.078 (2)–2.104 (2) Å and 90±4.42 (9)° for (II), and 2.0106 (17)–2.0555 (18) Å and 90±5.60 (7)° for (III).

Since one of the cations involved is Cu^{II}, the main differences are obviously found in the (Jahn–Teller-elongated) axial bonds, *viz.* 2.589 (3) and 2.8143 (6)–2.861 (2) Å for the Cu^{II}-containing complexes (I) and (III), respectively, *versus* 2.349 (2) Å for the Zn^{II}-containing complex (II). Fig. 4 presents a least-squares fit of the *L* coordination planes,

Table 2
Hydrogen-bond geometry (Å, °) for (I).

D—H···A	D—H	H···A	D···A	D—H···A
N1—H1N···O1^{i}	0.91	2.37	3.266 (6)	170
N2—H2N···O3^{i}	0.91	2.48	3.293 (5)	149
C7—H71···O2	0.96	2.37	3.296 (6)	162
C3—H32···O4^{ii}	0.97	2.48	3.448 (5)	177
C5—H52···O4^{iii}	0.97	2.48	3.126 (5)	124

Symmetry codes: (i) $-x+1, -y+1, -z+1$; (ii) $-x+\frac{1}{2}, y-\frac{1}{2}, -z+\frac{1}{2}$; (iii) $x+1, y, z$.

Table 3
Hydrogen-bond geometry (Å, °) for (II).

D—H···A	D—H	H···A	D···A	D—H···A
N1—H1N···O2^{i}	0.91	2.11	2.983 (5)	159
C7—H71···O1	0.96	2.38	3.245 (4)	150
N2—H2N···O3^{ii}	0.91	2.16	3.024 (4)	159

Symmetry codes: (i) $-x+\frac{1}{2}, -y+\frac{1}{2}, -z+1$; (ii) $x-\frac{1}{2}, -y+\frac{1}{2}, z-\frac{1}{2}$.

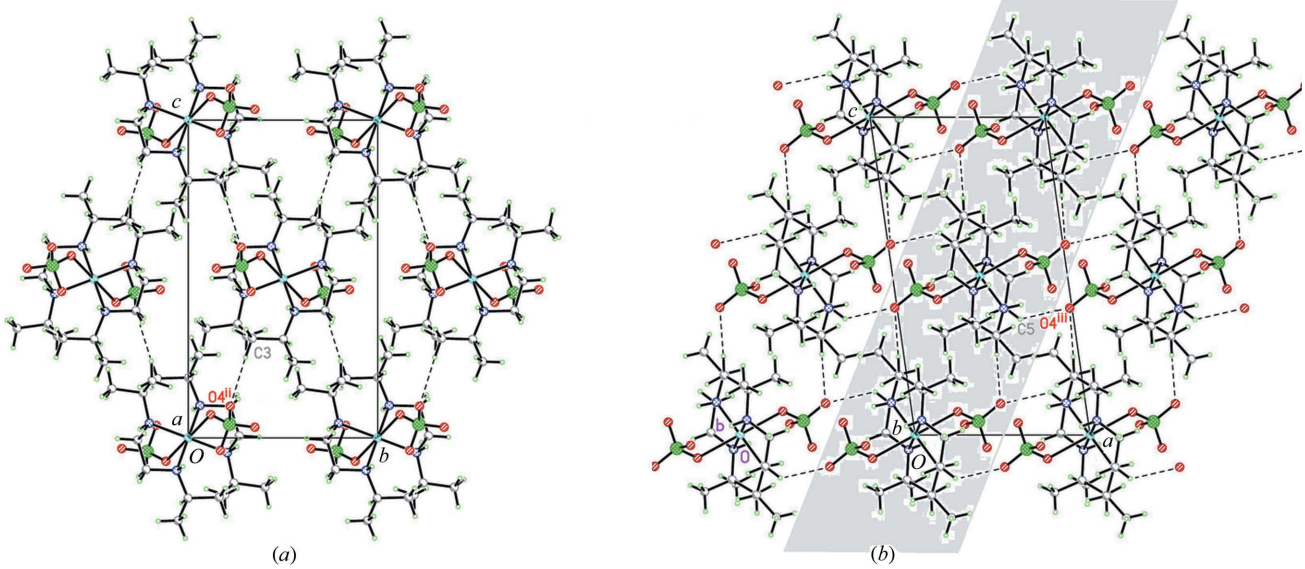

Figure 5
Packing views of (I), (*a*) along [100], showing the broad (100) plane determined by the C3—H32···O4^{ii} hydrogen bond, and (*b*) along [010], with planes (connected by the C5—H52···O4^{iii} hydrogen bond) shown sideways. One of the planes has been highlighted for clarity. [Symmetry codes: (ii) $-x+\frac{1}{2}, y-\frac{1}{2}, -z+\frac{1}{2}$; (iii) $x+1, y, z$.]

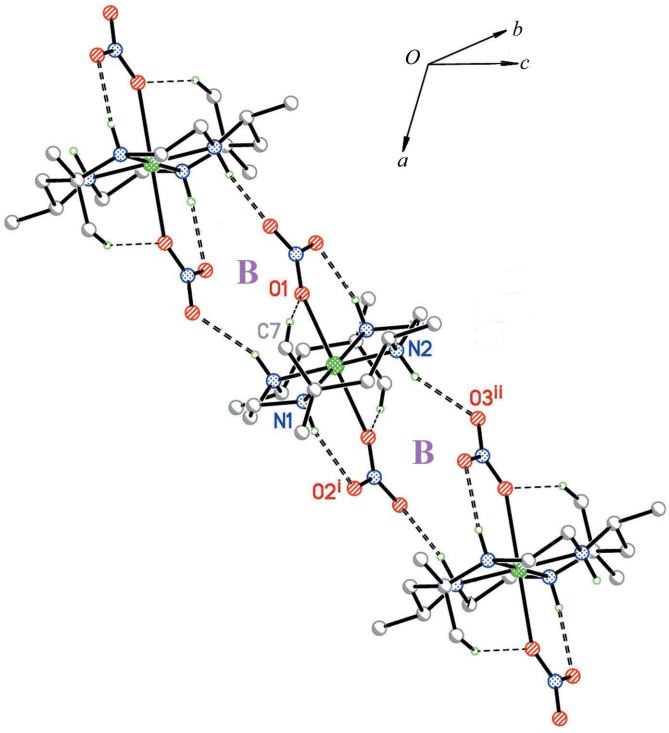

Figure 6
A packing view of (II), showing the one-dimensional chain running in the [101] direction. Double (single) broken lines denote conventional (nonconventional) hydrogen bonds. Label B corresponds to the $R_2^2(12)$ ring defined by the intermolecular N—H···O hydrogen bond. Symmetry codes as in Table 3.

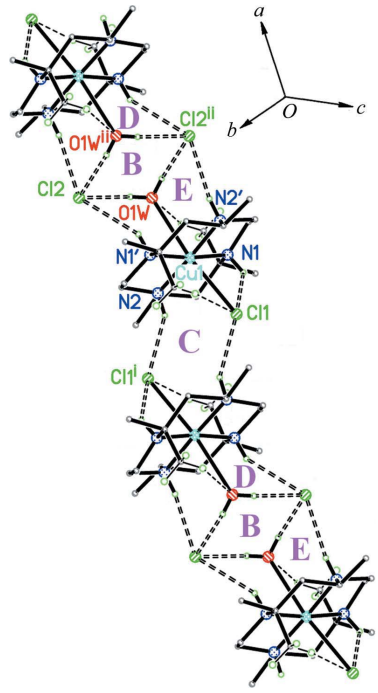

Figure 7
A packing view of (III), showing the one-dimensional chain running in the [100] direction. Double (single) broken lines denote conventional (nonconventional) hydrogen bonds. Symmetry codes as in Table 4.

confirming that the molecular differences reside mainly in the orientation and bonding distances of the axial ligands. We shall see below the impact this has on the hydrogen-bonding schemes.

The 14-membered rings have the usual zigzag shape and present four equatorial and two axial methyl groups, the latter being *trans* to each other. Amine atoms N1 and N2 [and N1′ and N2′ in (III)] present their H atoms on the same side of the coordination plane and opposite to the neighbouring axial methyl group. Due to coordination, the 14-membered ligand generates four smaller rings, two six-membered ones in chair conformations and two five-membered ones in half-chair forms. There are six chiral centres in the *L* ligand (N1/N1′, C4/C4′ and N2/N2′), in an *SR–RS–SR* configuration.

Table 4
Hydrogen-bond geometry (Å, °) for (III).

D—H···*A*	*D*—H	H···*A*	*D*···*A*	*D*—H···*A*
N1—H1N···Cl1	0.91	2.52	3.135 (2)	125
C7—H73···O1*W*	0.96	2.48	3.400 (4)	161
C7′—H71′···Cl1	0.96	2.75	3.697 (3)	170
N2—H2N···Cl1^{i}	0.91	2.55	3.369 (2)	149
N1′—H1N′···Cl2	0.91	2.70	3.531 (2)	152
N2′—H2N′···Cl2^{ii}	0.91	2.46	3.361 (2)	171
O1*W*—H1*WA*···Cl2	0.85 (2)	2.30 (2)	3.123 (3)	165 (2)
O1*W*—H1*WB*···Cl2^{ii}	0.84 (2)	2.40 (2)	3.204 (3)	160 (3)

Symmetry codes: (i) $-x+1, -y+1, -z+1$; (ii) $-x, -y+1, -z+1$.

In the same way, the different characteristics and orientations of the axial ligands lead to different orientations between hydrogen-bonding donors and acceptors, either facilitating or hampering intramolecular interactions.

In the case of (I), the perchlorate ligand coordinates to the cation through one of its O atoms (O2), leaving three potentially good acceptors ready for hydrogen bonding. The anionic group, which pivots on atom O2 and leans towards *L*, facilitates a double hydrogen-bonding interaction involving amine atoms N1 and N2 (Table 2, first and second entries), defining two $R(6)$ rings (labelled A and B in Fig. 1; for details of graph-set notation, see Bernstein *et al.*, 1995), and a weaker C—H···O interaction (third entry), all of which have the double effect of strongly binding the anion to the molecule while cancelling any possibility of strong intermolecular hydrogen bonds due to saturation of all suitable N—H donors. The result is a weak three-dimensional supramolecular structure sustained by weak hydrogen bonds involving two different C—H groups and free atom O4 (Table 2, fourth and fifth entries). The first of these describes the interaction defining broad (100) planes (Fig. 5*a*), while the second corresponds to the hydrogen bond which links planes together along [100] (Fig. 5*b*) to form the final three-dimensional structure. A very similar effect has been observed in the octamethylated counterpart of (I), $[Cu^{II}(ClO_4)_2(L^1)]$ (Nath *et al.*, 2013).

In (II), the ligand is the planar nitrate anion which binds the Zn^{II} cation through atom O1, thus leaving only two possible active O atoms. Of these, atom O2 appears in a favourable position for an intramolecular hydrogen bond with amine atom N1^{i} [symmetry code: (i) $-x+\frac{1}{2}, -y+\frac{1}{2}, -z+1$; Table 3, first entry], generating the usual $R(6)$ ring (A in Fig. 2). There

is in addition a weak C—H···O interaction (Table 3, second entry) completing the scheme of intramolecular contacts. As a consequence, amine atom N2 remains free to act as a donor and atom O3 as an acceptor for a single significant intermolecular interaction (Table 3, third entry) defining [101] chains. Fig. 6 shows details of this one-dimensional structure, which embeds inversion centres at the cation sites, and perpendicular twofold axes at the centres of the $R_2^2(12)$ loops (B in Fig. 6).

Finally, structure (III) presents a disrupting variant. The molecule is not centrosymmetric and there are two different axial ligands, one chloride anion (Cl1) and one neutral aqua ligand, which provides two efficient hydrogen-bond donors (H1*WA* and H1*WB*). There is, in addition, a second (noncoordinating) chloride counter-anion (Cl2). The intramolecular scheme is rather similar to that in (II), with amine atom N1 making a hydrogen bond to one axial ligand (Table 4, first entry), defining a tight $R(4)$ ring A (Fig. 3), and two weaker C—H···*X* hydrogen bonds (*X* = Cl or O; Table 4, second and third entries) completing the intramolecular scheme. This leaves amine atoms N2, N1′ and N2′ (now all independent) free to act as intermolecular hydrogen-bond donors in conjunction with the aqua H atoms, while having the chloride anions as acceptors. As a result, a number of linking hydrogen-bonded rings appear, *viz*. two of them noncentrosymmetric [B and D, both $R_2^1(8)$] and two centrosymmetric [C is $R_2^2(8)$ and E is $R_4^2(8)$], giving rise to the strongly connected [100] chain shown in Fig. 7.

The present discussion shows that the most significant difference in the hydrogen-bonding schemes in these three examples resides in the stronger (or weaker) acceptor character of the axial ligand(s) involved. In the case of (I), with its three available acceptor sites, all strong hydrogen-bonding donors in the macrocycle are saturated in intramolecular interactions, with the weak intermolecular contacts evenly distributed, and this provides for a smooth three-dimensional linkage. In (II) and (III), instead, there are N—H (and O—H) donors left over for intermolecular interactions, giving rise to the formation of strongly linked, though weakly interacting, chains.

The authors acknowledge ANPCyT (project No. PME 2006-01113) for the purchase of the Oxford Gemini CCD diffractometer, and also the University Grant Commission (UGC), Bangladesh, for a research grant to TGR.

Supplementary data for this paper are available from the IUCr electronic archives (Reference: SK3501). Services for accessing these data are described at the back of the journal.

References

Arai, H., Matshima, Y., Eguchi, T., Kazutoshi, S. & Katsumi, K. (1998). *Tetrahedron Lett.* **39**, 3181–3184.

Bakac, A. & Espenson, J. H. (1990). *Inorg. Chem.* **29**, 2062–2067.

Bernhardt, P. V. & Lawrance, G. A. (1990). *Coord. Chem. Rev.* **104**, 297–343.

Bernstein, J., Davis, R. E., Shimoni, L. & Chang, N.-L. (1995). *Angew. Chem. Int. Ed. Engl.* **34**, 1555–1573.

Curtis, N. F. (2012). *Coord. Chem. Rev.* **256**, 878–895.

Gao, Z., Tian, G., Zhao, G. & Si, C. (2010). *Inorg. Chem. Commun.* **13**, 461–463.

Hollinshead, A. C. & Smith, P. K. (1990). *Antibiot. Annu.* **313**, 1959–1960.

Kalita, A., Kumar, P., Deka, R. C. & Mondal, B. (2011). *Inorg. Chem.* **50**, 11868–11876.

Kimura, E., Bu, X., Shionoya, M., Wada, S. & Maruyama, S. (1992). *Inorg. Chem.* **31**, 4542–4546.

Kimura, E., Wada, S., Shionoya, M. & Okazai, Y. (1994). *Inorg. Chem.* **33**, 770–778.

Konig, B., Pelka, M., Zieg, H., Jones, P. G. & Dix, I. (1996). *Chem. Commun.* pp. 471–472.

Nath, B. C., Suarez, S., Doctorovich, F., Roy, T. G. & Baggio, R. (2013). *Acta Cryst.* C**69**, 689–695.

Norman, T. J., Parker, D., Smith, F. C. & King, D. J. (1995). *J. Chem. Soc. Chem. Commun.* pp. 1879–1880.

Oxford Diffraction (2009). *CrysAlis PRO*. Oxford Diffraction Ltd, Yarnton, Oxfordshire, England.

Reid, G. & Schroder, M. (1990). *Chem. Soc. Rev.* **19**, 239–269.

Roy, T. G., Hazari, S. K. S., Dey, B. K., Meah, H. A., Rahman, M. S., Kim, D. I. & Park, Y. C. (2007). *J. Coord. Chem.* **40**, 1567–1578.

Roy, T. G., Hazari, S. K. S., Dey, B. K., Miah, H. A., Olbrich, F. & Rehder, D. (2007). *Inorg. Chem.* **46**, 5372–5380.

Roy, T. G., Hazari, S. K. S., Dey, B. K., Nath, A., Anwar, N., Kim, D. I., Kim, E. H. & Park, Y. C. (2007). *J. Inclusion Phenom. Macrocycl. Chem.* **58**, 249–255.

Sheldrick, G. M. (2008). *Acta Cryst.* A**64**, 112–122.

Spek, A. L. (2009). *Acta Cryst.* D**65**, 148–155.

Suh, M. P., Moon, H. R., Lee, E. Y. & Jang, S. Y. (2006). *J. Am. Chem. Soc.* **128**, 4710–4718.

Temple, R., House, D. A. & Robinson, W. T. (1984). *Acta Cryst.* C**40**, 1789–1791.